in magnetically ordered crystals and light in cholesteric liquid crystals (Dmitrienko & Belyakov, 1977).

References

BECKER, P. (1977). Acta Cryst. A33, 243–249.
BORN, M. & WOLF, E. (1964). Principles of Optics. Oxford: Pergamon Press.
CHANDRASEKHAR, S. (1950). Radiative Transfer. Oxford: Clarendon Press.
CHANDRASEKHAR, S. (1960). Adv. Phys. 9, 363–386.
CODLING, K. (1973). Rep. Prog. Phys. 36, 541–624.
COHEN, G. G. & KURIYAMA, M. (1978). Phys. Rev. Lett. 40, 957–960.
DARWIN, C. G. (1922). Philos. Mag. 43, 800–829.
DMITRIENKO, V. E. & BELYAKOV, V. A. (1977). Zh. Eksp. Teor. Fiz. 73, 681–691. (Sov. Phys. – JETP, 46, 356–362.)
HART, M. (1978). Philos. Mag. B38, 41–56.

JENNINGS, L. D. (1968). Acta Cryst. A24, 472–474.
KATO, N. (1976). Acta Cryst. A32, 458–466.
LANDAU, L. D. & LIFSHITZ, E. M. (1958). Quantum Mechanics. Reading, Mass.: Addison-Wesley.
MIKHAJLJUK, I. P., KSHEVETSKIJ, S. A., OSTAPOVICH, M. V. & SHAFRANJUK, V. P. (1977). Ukr. Fiz. Zh. (Ukr. Ed.), 22, 61–64.
OLEKHNOVICH, N. M. & MARKOVICH, V. L. (1978). Kristallografiya, 23, 658–661.
OLEKHNOVICH, N. M., RUBTSOV, V. A. & SHMIDT, M. P. (1975). Kristallografiya, 20, 796–802.
PINSKER, Z. G. (1978). Dynamical Scattering of X-rays in Crystals. Berlin: Springer Verlag.
ROZENBERG, G. V. (1977). Usp. Fiz. Nauk, 121, 97–138.
SKALICKY, P. & MALGRANGE, C. (1972). Acta Cryst. A28, 501–507.
VAILLANT, F. (1977). Acta Cryst. A33, 967–970.
YAKIMENKO, M. N. (1974). Usp. Fiz. Nauk, 114, 55–66.
ZACHARIASEN, W. H. (1967). Acta Cryst. 23, 558–564.

Direct Analysis of Nuclear Distributional Moments in Zinc*

BY AINO VAHVASELKÄ

Department of Physics, University of Helsinki, Siltavuorenpenger 20 D, SF-00170 Helsinki 17, Finland

Abstract

The direct-analysis formalism of Kurki-Suonio [e.g. Isr. J. Chem. (1977), 16, Nos. 2–3, 115–123, 132–136] is modified to apply to the calculation of nuclear distributional moments $\langle x^\lambda y^\mu z^\nu \rangle$, which are linear combinations of the multipole moments $\langle r^k y_{lmp} \rangle$. They are integrated from the radial coefficients of the corresponding multipole terms through Gaussian and difference series procedures. An application to the thermal neutron diffraction structure factors of Merisalo & Larsen [Acta Cryst. (1977), A33, 351–354] on zinc indicates that the moment $\langle x^2 \rangle$ agrees with the anharmonic result of Merisalo & Larsen. $\langle z^2 \rangle$ does not show discrepancy with the value based on harmonic assumption. The existence of the third-order component in the nuclear smearing function and, due to this, anharmonicity of thermal motion is well established, but the magnitude of $\langle x^3 \rangle$ is not accurately defined on the basis of the present data. The ratios of the fourth and second moments do not reveal deviation from harmonic thermal smearing.

---

1. Introduction

The study of nuclear distributional moments by direct analysis in this work is intended to deal with deformation of harmonic nuclear smearing in hexagonal close-packed zinc. The non-centrosymmetric positions of the Zn atoms offer a possibility to study anharmonicity beyond merely centrosymmetric contributions. The direct-analysis formalism applied has been developed from the principles in studies concerning electronic charge and nuclear density distributions presented by Kurki-Suonio and his collaborators (e.g. Kurki-Suonio & Meisalo, 1967; Kurki-Suonio & Ruuskanen, 1971; Kurki-Suonio, Merisalo, Vahvaselkä & Larsen, 1976).

Merisalo & Larsen (1977) (hereafter M & L) have recently performed elastic neutron scattering measurements of the structure factors of Zn in order to study anharmonicity of lattice vibrations by a parameter-fitting procedure. The insufficiency of a harmonic formalism to explain thermal vibrations in crystals has caused vivid interest to focus on anharmonicity. This phenomenon seems to be amenable to study by several different methods as summarized by Willis & Pryor (1975), and indicated by the studies of Whiteley, Moss & Barnea (1978); Merisalo, Järvinen & Kurittu (1978);

Merisalo, Peljo & Soininen (1978); Merisalo & Järvinen (1978) and Kurki-Suonio, Merisalo & Peltonen (1979). The references mentioned conduct the analysis in terms of some modifications of parameter fitting.

We use the structure factors of M & L as experimental data. Besides a mere demonstration of the applicability of direct analysis to the calculation of relevant moments of nuclear distribution the choice of the Zn data of M & L as our object has another motive in a comparative and complementary study of anharmonicity. Direct analysis and parameter fitting are fundamentally different means of working with experimental data, though the leading theme in the treatments of the structure factors of zinc by M & L and us is the use of site-symmetrized expansions of real spherical harmonics for the effective potential and the nuclear density, respectively.

2. Direct analysis

The nuclear density distribution $s(\mathbf{r})$ of a crystal atom and the physical spatial observables connected with it obey the site symmetry of the particular atom, which means one of the 32 crystal point symmetries. To make this behaviour formally explicit $s(\mathbf{r})$ is expressed as a multipole expansion (Kurki-Suonio, 1977a):

$$s(\mathbf{r}) = \sum_{lmp} \frac{1}{N_{lmp}} s_{lmp}(r) y_{lmp}(\theta, \varphi), \qquad (1)$$

where the origin is at the atomic position studied, a local Cartesian coordinate system adapted to the site symmetry is applied and the real spherical harmonics,

$$y_{lmp} = y_{lm\pm} = P_l^m(\cos\theta) \frac{\cos m\varphi}{\sin m\varphi},$$

$$l = 0, 1, \ldots; \ m = 0, 1, \ldots, l, \qquad (2)$$

with the normalization

$$N_{lmp}^2 = \int_{(4\pi)} |y_{lmp}|^2 \, d\Omega = (1 + \delta_{m0}) \frac{2\pi}{2l+1} \frac{(l+m)!}{(l-m)!}, \qquad (3)$$

are chosen according to the requirements of site symmetry.

The nuclear distribution $s(\mathbf{r})$ is assumed to be a superposition of weighted nuclear smearing functions τ_n (Kurki-Suonio, Merisalo, Vahvaselkä & Larsen, 1976)

$$s(\mathbf{r}) = \sum_n g_n \tau_n(\mathbf{r} - \mathbf{r}_n), \qquad (4)$$

where the summation runs over all the atoms of the crystal, g_n and $\mathbf{r}_n$ are the nuclear scattering amplitude and the position of the nth atom. Due to this superposition model the structure factor has the familiar form

$$G(\mathbf{b}_\nu) = \sum_n g_n T_n(\mathbf{b}_\nu) \exp(2\pi i \mathbf{b}_\nu \cdot \mathbf{r}_n), \qquad (5)$$

where n runs over the atoms of the unit cell and T_n is the Fourier transform of the thermal smearing function τ_n.

The assumption that the nuclear thermal motion corresponds to a harmonic potential field leads to a Gaussian smearing function, which produces a Gaussian temperature factor. We introduce it in the well known form

$$T(\mathbf{b}) = \exp[-2\pi^2(B_1 \eta^2 + B_2 \kappa^2 + B_3 \mu^2)], \qquad (6)$$

where B_i equals $\langle u_i^2 \rangle$, $i = 1, 2, 3$, the mean square displacement of the atom along the principal axis i, and η, κ, μ represent the scattering vector $\mathbf{b}$ in the Cartesian coordinate system defined by the principal axes.

The experimental information available for the calculation of any quantities describing the nuclear density distribution is contained in the structure factors G_ν obtained from Bragg diffraction experiments with thermal neutrons. In direct analysis we choose to consider quantities X that can be expressed as sums

$$X = \sum_\nu c_\nu G_\nu, \qquad (7)$$

where the summation is over the reciprocal lattice $\{\mathbf{b}_\nu\}$.

In the direct analysis of X-ray data the residual-term problem in connection with the series (7) has been settled by assuming harmonic behaviour of the temperature factor above the cutoff limit. The values of the B_i parameters have been fixed by the criterion of natural continuation of the experimental atomic factors over the cutoff limit in $\mathbf{b}$ space (Kurki-Suonio & Fontell, 1964; Vahvaselkä & Kurki-Suonio, 1975). This is realized by making the radial difference densities Δs_{lmp}, $l = 0, 2$, in difference multipole expansion (1) flat at the origin. This is achieved by adjusting the B_i values of the temperature factor (6) in G_{calc} to make the second derivatives of the radial monopole and quadrupole difference densities zero at the origin (Kurki-Suonio, 1977b). Here the series representation (8) is used for Δs_{lmp} with the coefficients $\Delta G_\nu = G_{\nu,\text{obs}} - G_{\nu,\text{calc}}$ below the cutoff and $\Delta G_\nu = 0$ beyond it. The application of this procedure to neutron diffraction data means that we assume the anharmonicity of the smearing to vanish asymptotically at large $(\sin\theta)/\lambda$.

3. Moments of nuclear distribution

A representation of the behaviour for small enough values of r of the radial coefficient $s_{lmp}(r)$ in (1) of a crystal atom can be obtained (Kurki-Suonio, 1967) in terms of structure factors as

$$s_{lmp}(r) = \frac{4\pi(-i)^l}{V N_{lmp}} \sum_\nu G_\nu j_l(2\pi b_\nu r) y_{lmp}(u_\nu, v_\nu), \qquad (8)$$

where V is the volume of the unit cell, b, u, v are the spherical coordinates in reciprocal space, and the phases of the structure factors G_v are given with respect to the origin at the nucleus for which the calculation is performed.

Although $s_{lmp}(r)$, especially $s_0(r)$, may give a concrete view of the distribution around the nuclear position, the reliability of the radial densities is not as good as that of integrated quantities (Kurki-Suonio, 1971). Equation (7) indicates that the sooner the coefficient $c_v(b)$, called 'the reciprocal distribution' of X approaches zero the less the quantity is dependent on the structure factors with high b values. The examples given by Kurki-Suonio (1971) indicate that the reciprocal distribution of integrated quantities behaves more favourably in this respect than that of radial distributions $s_{lmp}(r)$.

We define the nuclear distributional moments (multipole moments) as the expectation values

$$\langle r^k y_{lmp} \rangle = \frac{\int s(\mathbf{r}) r^k y_{lmp} \, d^3 r}{\int s(\mathbf{r}) \, d^3 r} = \frac{1}{g} \int s(\mathbf{r}) r^k y_{lmp} \, d^3 r, \quad (9)$$

where we integrate over the whole space and denote the integral $\int s(\mathbf{r}) \, d^3 r$ by g. After the insertion of the multipole expansion (1) in (9) we get

$$\langle r^k y_{lmp} \rangle = \frac{N_{lmp}}{g} \int_0^\infty s_{lmp}(r) r^{k+2} \, dr, \quad (10)$$

where the orthogonality of the harmonics y_{lmp} has been made use of. $\langle r^k y_{lmp} \rangle$ is a parameter calculable directly from the series (7) since on inserting (8) in (10) it can be written as

$$\langle r^k y_{lmp} \rangle = \frac{4\pi(-i)^l}{Vg} \sum_v G_v y_{lmp}(u_v, v_v)$$

$$\times \int_0^R j_l(2\pi b_v r) r^{k+2} \, dr. \quad (11)$$

The lowest possible value which k can assume here is $k = -l - 2$ (Kurki-Suonio, 1971).

In writing in (11) the upper limit of integration as R instead of infinity we assume the nuclear smearing of the atom considered to be contained within a sphere of radius R. This spherical volume partitioning (SVP) method, as it is called by Dawson (1975), is based on the assumption of locality of the atoms (Kurki-Suonio & Salmo, 1971). As regards the nuclear smearing functions, SVP is certainly better justified than in the case of charge densities, and we expect no significant contributions from neighbouring atoms in the sphere that already contains the whole smearing function of the atom at hand. This means that all multipole moments (11) must saturate at a certain radius R.

If the experimental value of the multipole moment is desired the evaluation of the residual term in the expansion (11) is necessary. The procedure applied is

equivalent to approximating the experimental structure factors in the residual-term region by a harmonic model. The series (11) is used in practice as a difference series with $\Delta G_v = G_{v,\text{obs}} - G_{v,\text{calc}}$ as coefficients up to the cutoff in b and zero beyond that. Experimental distributional moments are obtained by adding the results given by the difference series to the moments of the Gaussian nuclear distribution (6) of the relevant atom. No corrections due to the tails of neighbouring distributions are needed because of the good separation of the nuclei in the crystal. This procedure is an extension of the method of Hosemann & Bagchi (1962) for charge densities. It has been applied before in direct-analysis formalism in the calculation of radial charge densities (e.g. Kurki-Suonio & Ruuskanen, 1971) and electron counts in spheres (Kurki-Suonio & Salmo, 1971). To obtain a Gaussian multipole moment $\langle r^k y_{lmp} \rangle$ for the atom n the Fourier transform of $g_n T_n(\mathbf{b})$ is inserted for $s(\mathbf{r})$ in (9), where the integration is extended over the atomic sphere of radius R. We perform the calculation of the multipole moments as a function of R. In order to obtain characteristic values of the moments for the atoms studied we apply the assumption of saturation stated above. The validity of the assumption of locality (and the goodness of data) will then appear in the degree of saturation. In the case of good saturation a well defined experimental value of the moment follows. A poor saturation will indicate inaccuracy of the moment as defined by the data.

Suitable linear combinations of the $\langle r^k y_{lmp} \rangle$ quantities can be conveniently used to characterize the thermal motion of nuclei in crystals. We shall particularly apply them in the study of anharmonicity. We limit this study on atoms located at unit-cell positions exactly specified by symmetry. Site symmetry indicates what moments to look for. A general Gaussian smearing function (6) possesses all the multipole moments $lm+$ with l and m even. For an axial one with $B_1 = B_2$ all the moments with $m \neq 0$ vanish (and for a spherical one both l and m must be zero). Appearance of any other multipoles, if allowed by the site symmetry, will serve as direct indication of anharmonicity. Anharmonicity will also change the relations of the moments from the values fixed by the harmonic model.

4. Application to zinc

Zinc crystallizes according to the crystallographic space group $P6_3/mmc$ (No. 194) with two atoms per unit cell in the special positions $\frac{1}{3}, \frac{2}{3}, \frac{1}{4}$ (A) and $\frac{2}{3}, \frac{1}{3}, \frac{3}{4}$ (B) related by inversion. Zn has a hexagonal close-packed structure with unit-cell dimensions $a = b = 2\cdot664$ and $c = 4\cdot945$ Å. The local Cartesian coordinate axes conform to the $\bar{6}m2$ site symmetry of the atoms by making the z axis $\parallel \bar{6}$, the y axis $\perp m$ and the x axis $\parallel 2$ as indicated in Fig. 1 for the atom A.

The indices *lmp* of the spherical harmonics y_{lmp} in the multipole expansion (1) are allowed to have the values $(m + 2j, 3\mu, +)$, μ and j any integers such that $l \geq m \geq 0$ (Kurki-Suonio, Merisalo & Peltonen, 1979). We shall consider the monopole, quadrupole, octupole and hexadecapole terms with $lmp = 00+, 20+, 33+, 40+$.

The experimental data in our analysis are the room-temperature single-crystal thermal neutron diffraction structure factors of M & L scaled and corrected for extinction to a harmonic model by least-squares fitting. M & L omit the reflexions 100 and 110 from their calculations. The checking of the scale of the structure factors and the asymptotic para-metrization of the nuclear smearing model indicate slight changes to the parameters of M & L. The g_n and r_n parameters naturally remain the same, $g_n = 0.57 \times 10^{-14}$ m (Bacon, 1972) and the position parameters r_n as given above, also the equality of B_{n1} and B_{n2} remains due to symmetry, but the experimental structure factors of M & L have to be multiplied by 0·993 and $B_{n1} = B_{n2}$ and B_{n3} have to be changed to $B_{n1} = B_{n2} = 0·0111$ Å^2 and $B_{n3} = 0·0276$ Å^2. Table 1 lists the experimental structure factors G_{obs} modified as to the scale and referred to the origin of the unit cell applied here, their standard deviations σ and the theoretical harmonic structure factors G_{calc}.

The natural displacement quantities connected with a zinc nucleus are the mean square deviations $\langle x^2 \rangle$ and $\langle z^2 \rangle$. The cubic and quartic mean deviations $\langle x^3 \rangle$, $\langle x^4 \rangle$, $\langle z^4 \rangle$, $\langle x^2 z^2 \rangle$, also naturally arise due to symmetry. Table 2 indicates how the expectation values $\langle r^k y_{lmp} \rangle$ are worked on to yield the desired results. In order to obtain the experimental moments we proceed through the Gaussian difference-series calculations as presented in the previous chapter.

Figs. 2, 3 and 4 present the moments as functions of R, the radius of the sphere of integration. The standard deviations are deduced on the basis of the errors given in Table 1. Fig. 2 of the second moments gives the ultimate limits of the mean square deviations according to the harmonic and anharmonic models of M & L. Fig. 3 gives the limits connected with the quartic deviations
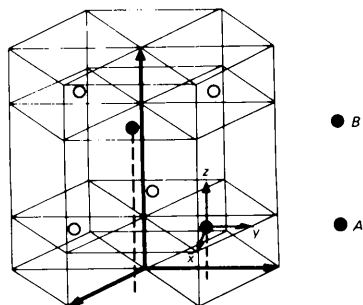
Table 1. *The experimental structure factors of zinc, their experimental standard deviations and the theoretical structure factors calculated according to equation* (5)

h k l	$b = 2(\sin \theta)/\lambda$ [Å^{-1}]	G_{obs}	σ	G_{calc}
0 0 2	0·40444	−1·052	0·005	−1·043
0 0 4	0·80890	0·795	0·004	0·799
0 0 6	1·21334	−0·498	0·003	−0·512
1 0 1	0·47830	−0·939	0·005	−0·927
1 0 2	0·59284	0·502	0·003	0·501
1 0 3	0·74560	0·776	0·004	0·776
1 0 4	0·91770	−0·378	0·002	−0·383
1 0 5	1·10012	−0·535	0·003	−0·543
1 0 6	1·28844	0·244	0·001	0·246
1 0 7	1·48044	0·312	0·002	0·319
1 1 2	0·85276	−0·930	0·005	−0·922
1 1 4	1·10360	0·711	0·004	0·706
1 1 6	1·42682	−0·448	0·002	−0·453
2 0 0	0·86690	−0·472	0·002	−0·484
2 0 1	0·89016	0·808	0·004	0·819
2 0 2	0·95660	0·456	0·002	0·443
2 0 3	1·05810	−0·692	0·003	−0·686
2 0 4	1·18568	−0·343	0·002	−0·339
2 0 5	1·33186	0·481	0·002	0·481
2 0 6	1·49122	0·223	0·001	0·217
2 1 0	1·14680	−0·416	0·002	−0·428
2 1 1	1·16448	−0·716	0·004	−0·725
2 1 2	1·21602	0·397	0·002	0·391
2 1 3	1·29738	0·618	0·003	0·606
2 1 4	1·40336	−0·302	0·002	−0·300
2 1 5	1·52888	−0·431	0·002	−0·425
2 2 0	1·50150	0·679	0·003	0·697
2 2 2	1·55502	−0·643	0·003	−0·637
3 0 0	1·30034	0·745	0·004	0·788
3 0 2	1·36178	−0·725	0·004	−0·721
3 0 4	1·53140	0·559	0·003	0·552
3 1 0	1·56282	−0·340	0·002	−0·334

Fig. 1. The unit cell and the local Cartesian coordinate axes in a Zn crystal.
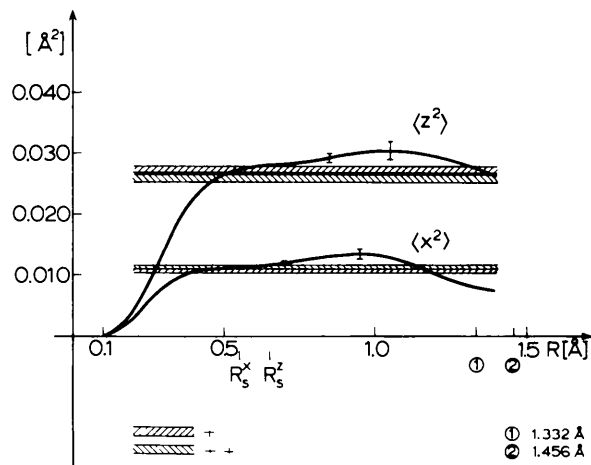

Fig. 2. The second moments of the nuclear density distribution in Zn. R_s^x and R_s^z are the radii for which $\langle x^2 \rangle$ and $\langle z^2 \rangle$ are evaluated. The circled 1 and 2 are the half-way points between an atom in the *xy* plane and the nearest one in and outside the *xy* plane. + Harmonic limits of M & L. + + Anharmonic limits of M & L.

Table 2. Moments of nuclear distribution in the $\bar{6}m2$ site symmetry of a Zn atom

$$\langle r^2 y_{00+} \rangle = \langle r^2 \rangle = \qquad\qquad 2\langle x^2 \rangle + \langle z^2 \rangle$$
$$\langle r^2 y_{20+} \rangle = \langle r^2 \tfrac{1}{2}(3\cos^2\theta - 1) \rangle = -\langle x^2 \rangle + \langle z^2 \rangle$$
$$\langle r^3 y_{33+} \rangle = \langle r^3 15 \sin^3\theta(4\cos^3\varphi - 3\cos\varphi) \rangle = 60\langle x^3 \rangle$$
$$\langle r^4 y_{00+} \rangle = \langle r^4 \rangle = \qquad\qquad \tfrac{3}{5}\langle x^4 \rangle + \langle z^4 \rangle + 4\langle x^2 z^2 \rangle$$
$$\langle r^4 y_{20+} \rangle = \langle r^4 \tfrac{1}{2}(3\cos^2\theta - 1) \rangle = \qquad -\tfrac{1}{7}\langle x^4 \rangle + \langle z^4 \rangle + \langle x^2 z^2 \rangle$$
$$\langle r^4 y_{40+} \rangle = \langle r^4 \tfrac{1}{8}(35\cos^4\theta - 30\cos^2\theta + 3)\rangle = \quad \langle x^4 \rangle + \langle z^4 \rangle - 6\langle x^2 z^2 \rangle$$

$$\langle x^2 \rangle = \tfrac{1}{3}\langle r^2 y_{00+} \rangle - \tfrac{1}{3}\langle r^2 y_{20+} \rangle$$
$$\langle z^2 \rangle = \tfrac{1}{3}\langle r^2 y_{00+} \rangle + \tfrac{2}{3}\langle r^2 y_{20+} \rangle$$
$$\langle x^3 \rangle = \tfrac{1}{60}\langle r^3 y_{33+} \rangle$$
$$\langle x^4 \rangle = \tfrac{1}{5}\langle r^4 y_{00+} \rangle - \tfrac{2}{7}\langle r^4 y_{20+} \rangle + \tfrac{3}{35}\langle r^4 y_{40+} \rangle$$
$$\langle z^4 \rangle = \tfrac{1}{5}\langle r^4 y_{00+} \rangle + \tfrac{4}{7}\langle r^4 y_{20+} \rangle + \tfrac{8}{35}\langle r^4 y_{40+} \rangle$$
$$\langle x^2 z^2 \rangle = \tfrac{1}{15}\langle r^4 y_{00+} \rangle + \tfrac{1}{21}\langle r^4 y_{20+} \rangle - \tfrac{4}{35}\langle r^4 y_{40+} \rangle$$

Symmetry implies the equalities $\langle x^2 \rangle = \langle y^2 \rangle$; $\langle xy \rangle = \langle xz \rangle = \langle yz \rangle = 0$; $\langle x^4 \rangle = \langle y^4 \rangle$; $\langle x^2 z^2 \rangle = \langle y^2 z^2 \rangle$; $\langle x_i x_j x_k^2 \rangle = 0$, $i \neq j \neq k$; $\langle x_i x_j^3 \rangle = 0$, $i \neq j$. Symmetry conditions lead to the relation $\langle x^2 y^2 \rangle = \tfrac{1}{3}\langle x^4 \rangle$. All the third moments equal zero identically, except $\langle x^3 \rangle$ and $\langle xz^2 \rangle$, for which $\langle x^3 \rangle = -\langle xy^2 \rangle$.

in Table 3 based on calculations using the anharmonic potential parameters of M & L.

The Gaussian model distribution approaches zero asymptotically and causes the model moments to behave regularly as functions of R but the Δs_{Imp} curves in (8), from which the experimental contributions to the moments are calculated, fluctuate around zero in the central region between the nuclei due to the series termination error and make the moments fluctuate too. The moments $\langle x^2 \rangle$, $\langle z^2 \rangle$, $\langle x^4 \rangle$, $\langle z^4 \rangle$ still display a clear saturation around the radius $R = 0.6$ Å. Also $\langle x^2 z^2 \rangle$ has an inflexion point at about this radius as an indication of saturation. We evaluate these moments at the points R_s, indicated in the figures, that visually best represent the concept of saturation, i.e. at the maximum of $\langle z^4 \rangle$ and at the inflexion points of the others. These regions of inflexion comply suitably with the behaviour of the spherical average nuclear distribution $s_{00+}(r)\, r^2 \int y_{00+}/N_{00+}\, d\Omega = s_{00+}(r)\, r^2\, 2\sqrt{\pi}$ in Fig. 5 calculated according to a Gaussian and a difference series procedure analogous to the one in this work. The

half-way points between an atom in the xy plane and the nearest one in and outside the xy plane are located at 1.332 and 1.456 Å. The significant parts of the moment curves occur far before these points are reached, which means that our results can be obtained
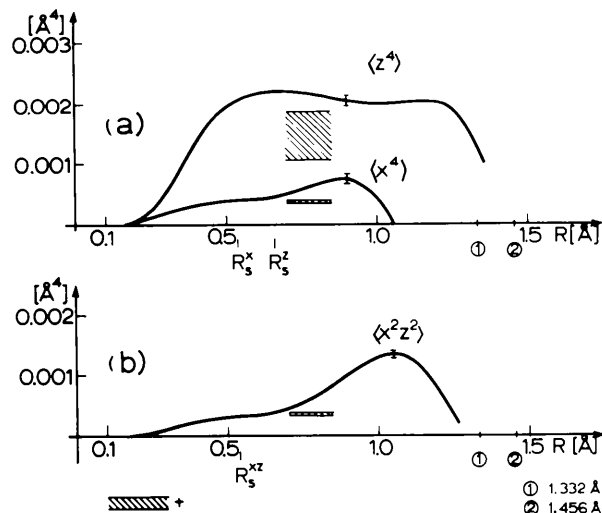

Fig. 3. The fourth moments of the nuclear density distribution in Zn and their radii of saturation R_s^x, R_s^z and R_s^{xz}. + Anharmonic limits of M & L.
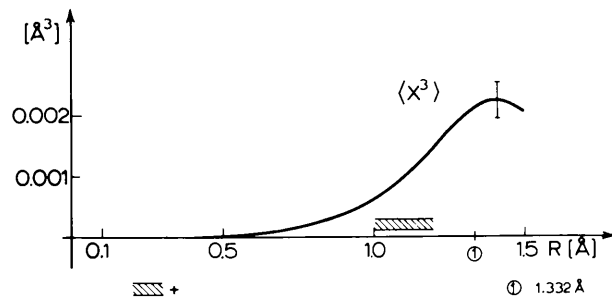

Fig. 4. The third moment of the nuclear density distribution in Zn. + Anharmonic limits from column 7, Table 3.

Table 3. Moments of nuclear distribution in Zn

Column 1. The radii of saturation. Column 2. Experimental moments of nuclear distribution in Zn and their standard deviations. The third moment is limited in the interval defined by the minimum and maximum R_s, 0·54 and 0·66 Å in column 1. Column 3. Uncertainty in the values of the moments due to the determination of the saturation points. Column 4. Gaussian limiting moments. Columns 5, 6. Moments of nuclear distribution obtained from the anharmonic models 1 and 2 of M & L. Column 7. Limits for the mean cubic deviation obtained from the parameters of M & L, Merisalo & Larsen (1979) and Merisalo, Järvinen & Kurittu (1978).

1 R_s [Å]	2 This work	3	4 Gaussian	5 M & L anharmonic 1	6 M & L anharmonic 2	7
0·55	$\langle x^2 \rangle = 0.0113\,(1)$ Å^2	(2) Å^2	0·0111 Å^2	0·0113 (3) Å^2	0·0114 (3) Å^2	
0·65	$\langle z^2 \rangle = 0.0279\,(3)$ Å^2	(3) Å^2	0·0276 Å^2	0·0260 (5) Å^2	0·0257 (5) Å^2	
–	0.000022 (2) Å^3 $< \langle x^3 \rangle <$ 0.000080 (8) Å^3	–	0 Å^3	0 Å^3	0 Å^3	0.000115 Å^3 $< \langle x^3 \rangle <$ 0.000325 Å^3
0·54	$\langle x^4 \rangle = 0.000388\,(4)$ Å^4	(26) Å^4	0·000370 Å^4	0·000372 (9) Å^4	0·000388 (6) Å^4	
0·66	$\langle z^4 \rangle = 0.00222\,(2)$ Å^4	(3) Å^4	0·00229 Å^4	0·00157 (30) Å^4	0·00145 (41) Å^4	
0·54	$\langle x^2 z^2 \rangle = 0.000312\,(1)$ Å^4	(31) Å^4	0·000306 Å^4	0·000371 (17) Å^4	0·000360 (18) Å^4	

within 'the requirement of locality' (Kurki-Suonio, 1968) of direct analysis.

Table 3 reports the radii R_s chosen for the saturation points and the corresponding experimental moments. The appearance of the moment curves induces some uncertainty in the values of the moments. For that reason Table 3 also gives the indeterminacy of the nuclear distributional moments obtained by evaluating the moments at $R_s \pm 0.05$ Å for the second moments and at $R_s \pm 0.06$ Å for the fourth moments.

The odd moment $\langle x^3 \rangle$ in Fig. 4 displays a different behaviour. It grows steeply and reaches a sharp maximum. This appearance does not permit any statement about the magnitude of the third moment to be made. We have limited its value in Table 3, column 2, between the values obtained at $R = 0.54$ and $R = 0.66$ Å, the minimum and maximum of the radii of saturation in column 1 of Table 3.

Table 3 includes the limiting Gaussian moments

$$\langle x^\lambda y^\mu z^\nu \rangle = \frac{1}{(2\pi)^{3/2} (B_1 B_2 B_3)^{1/2}} \int\limits_{-\infty}^{\infty} \int \int x^\lambda y^\mu z^\nu$$

$$\times \exp\left[-\frac{1}{2}\left(\frac{x^2}{B_1} + \frac{y^2}{B_2} + \frac{z^2}{B_3} \right) \right] dx \, dy \, dz$$

$$= \frac{(2B_1)^{\lambda/2} (2B_2)^{\mu/2} (2B_3)^{\nu/2}}{\pi^{3/2}}$$

$$\times \Gamma\left(\frac{\lambda+1}{2} \right) \Gamma\left(\frac{\mu+1}{2} \right) \Gamma\left(\frac{\nu+1}{2} \right), \quad (12)$$

where $\lambda + \mu + \nu = l$ and λ, μ, ν are even, otherwise $\langle x^\lambda y^\mu z^\nu \rangle = 0$.
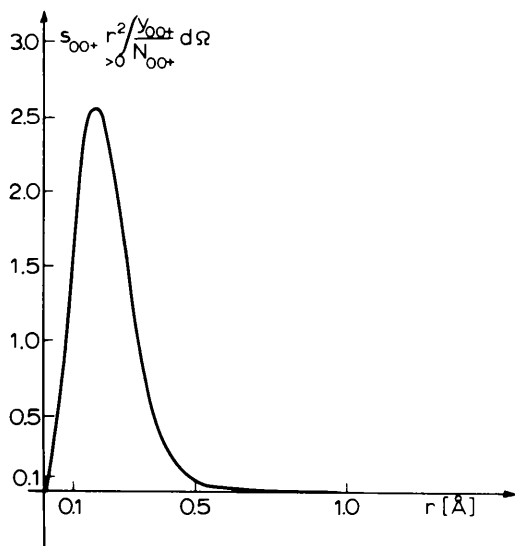

Fig. 5. The spherical average or monopole experimental nuclear density distribution. The experimental limits of error are so small that they hardly show in the scale of the figure.

Table 3 also includes the second moments of the anharmonic models 1 and 2 of M & L. We calculated the fourth moments of M & L using their potential parameters in the expansion of the potential V in their expression of an ensemble average

$$\langle x^\lambda y^\mu z^\nu \rangle = \frac{\int x^\lambda y^\mu z^\nu \exp\left[-V(\mathbf{r})/k_B T \right] dx \, dy \, dz}{\int \exp\left[-V(\mathbf{r})/k_B T \right] dx \, dy \, dz},$$
$$(13)$$

where k_B is the Boltzmann constant and T the absolute temperature equal to 295 K. The third moment $\langle x^3 \rangle$ equals exactly zero on the basis of the parameters of M & L. A value different from zero for $\langle x^3 \rangle$ is obtained by applying the result of the study of almost-forbidden reflexions 301 and 303 by Merisalo, Järvinen & Kurittu (1978). They determine a value of $a_{33} = -(1.50 \pm 0.5) \times 10^{-19}$ JÅ^{-3} for the force constant of the cubic term of the potential. Another value, $a_{33} = -(1.8 \pm 0.3) \times 10^{-19}$ JÅ^{-3}, is given by Merisalo & Larsen (1979) in their reconsideration of the same data as we have been referring to here. We obtain the limits for $\langle x^3 \rangle$ indicated in column 7 of Table 3 by applying the above a_{33} values and the parameters of the anharmonic models 1 and 2 of the potential expansion of M & L to a calculation of $\langle x^3 \rangle$ according to (13).

5. Discussion

The octupole term in the expansion of $s(\mathbf{r})$ (1) deforms the centrosymmetric smearing pattern. Harmonicity implies centrosymmetry, which is violated if the third moment really exists. The accuracy of the structure factors at our disposal is not sufficient to determine the minute $\langle x^3 \rangle$ better than qualitatively, but Fig. 4 would give for $\langle x^3 \rangle$ a value rather close to the values in the hatched region obtained as a result of parameter fitting, if we evaluate it at 0.6 Å, which approximately indicates the point of saturation of the second and fourth moments.

The search for the magnitude of $\langle x^3 \rangle$ motivates one to consider the quantity

$$s_{lmp}(r) r^2 \int\limits_{>0} \frac{y_{lmp}}{N_{lmp}} d\Omega = s_{lmp}(r) r^2 \int\limits_{\tau'} \frac{y_{lmp}}{N_{lmp}} d\Omega, \quad (14)$$

the radial density of nuclear smearing within the positive lobes τ' of the spherical harmonics. Its values are obtained by Gaussian and difference-series procedures analogous to the one applied in the calculation of the multipole moments. Fig. 6 represents the Gaussian and experimental functions (14) for $l = 0, 2, 3, 4$ in the interesting region of saturation of the moments. The Gaussian curves approach zero

asymptotically; that is for $l = 2, 4$ they extend as far as the monopole density. This is natural from the point of view of the higher components redistributing the contents of the monopole component. The experimental spherical average or monopole density displays negative values above 1 Å, which is not physically real.
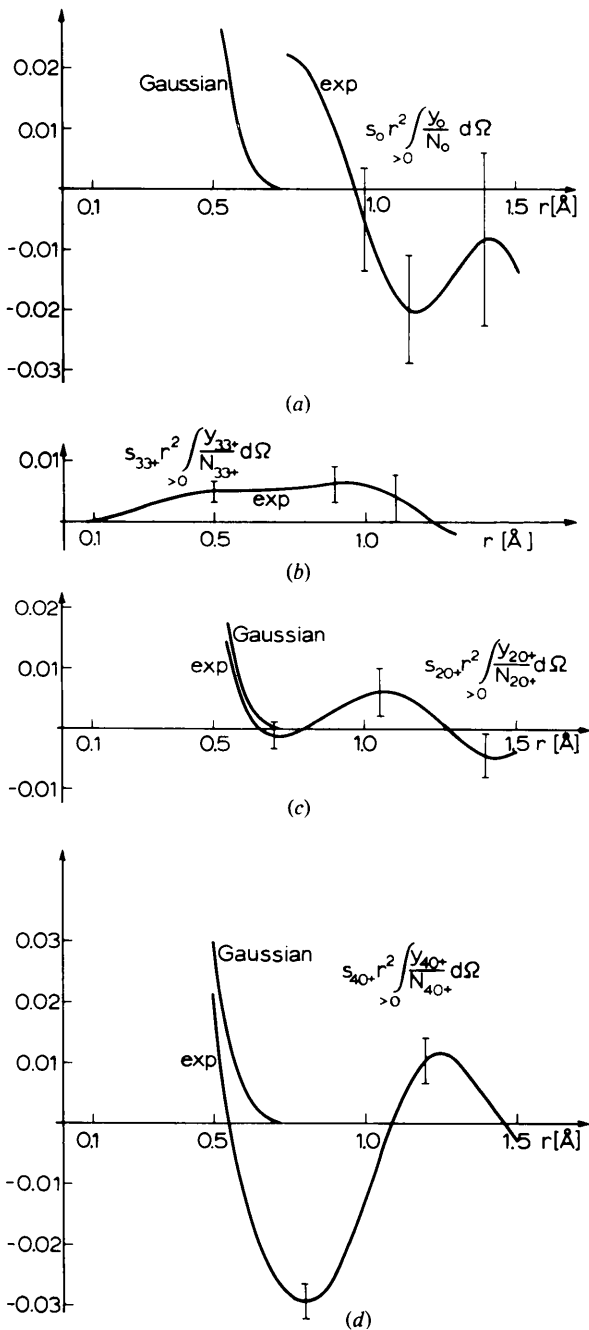

(a)

(b)

(c)

(d)

Fig. 6. (a) The spherical average or monopole experimental and Gaussian nuclear density distributions. (b) The octupole experimental nuclear density distribution. (c) The quadrupole and (d) the hexadecapole experimental and Gaussian nuclear density distributions.

Table 4. *Mean square deviations along the principal axes in Zn*

	$\langle x^2 \rangle$ |Å²|	$\langle z^2 \rangle$ |Å²|
Barron & Munn (1967) (B & M)	0·0085 (5)	0·0276 (15)
Skelton & Katz (1968) (S & K)	0·0112 (3)	0·0259 (10)
Rossmanith (1977) (Mo $K\alpha$)	0·0096 (2)*	
(Cu $K\alpha$)	0·0104 (12)*	0·0259 (13)*
Merisalo & Larsen (1977) (M & L)		
harmonic	0·0107 (3)	0·0273 (5)
anharmonic 1	0·0113 (3)	0·0260 (5)
anharmonic 2	0·0114 (3)	0·0257 (5)
Kurki-Suonio, Merisalo & Peltonen (1979) (K-S, M & P)		
harmonic	0·0109 (3)	0·0272 (5)
anharmonic	0·0113 (3)	0·0258 (5)
This work	0·0113 (1)	0·0279 (3)
	(2)†	(3)†

* Values deduced on the basis of the root-mean-square displacement values u_a and u_c of Rossmanith (1977).
† The uncertainty from column 3 of Table 3.

The fluctuation of the hexadecapole density is strong in the critical region of saturation of the fourth moments. This phenomenon diminishes the credibility of the fourth moments on the basis of the experimental data applied. Fig. 6 indicates that the region of saturation of the moments coincides with the values where the Gaussian distribution has considerably decreased and with the beginning of the waving character of the experimental density.

The positive octupole density in Fig. 6(b) extends further than the positive monopole density, which is unrealistic. However, the existence of the positive octupole density looks obvious in Fig. 6(b), but its numerical uncertainty seems greater than the standard limits of error indicate. The octupole density and the third moment in Fig. 4 qualitatively confirm the result of Merisalo, Järvinen & Kurittu (1978), who report softening of the effective one-particle potential in the x direction and hardening in the opposite direction, which indicates larger amplitude of vibration in the x direction than in the $-x$ direction.

In Table 4, mean square deviations along the principal axes are shown with results from several authors as well as this work. Barron & Munn (1967) (hereafter B & M) calculated their mean square deviations from thermodynamic data within the quasi-harmonic approximation of the temperature factor. The experimental results of Skelton & Katz (1968) (hereafter S & K) and Rossmanith (1977) were measured from single-crystal X-ray diffraction intensities. The values of M & L are quoted from their parameter-fitting-type analysis. Kurki-Suonio, Merisalo & Peltonen (1979) (hereafter K-S, M & P) contribute the results of their site-symmetrized treatment of anharmonic temperature factors concerning the same zinc data as in this work.

Our $\langle x^2 \rangle$ indicates a definite increase above the value of B & M and the best agreement with the experi-

mental result of S & K and the anharmonic results of M & L and K-S, M & P. Within the experimental limits of error and the indeterminacy in the evaluation of the moment our $\langle z^2 \rangle$ agrees best with the $\langle z^2 \rangle$ of B & M and the harmonic results of M & L and K-S, M & P. On the other hand the experimental result of S & K and the anharmonic results of M & L and K-S, M & P agree with each other, but because of the overlapping of the limits of error there is no definite inequality between the $\langle z^2 \rangle$ of B & M and the experimental and anharmonic $\langle z^2 \rangle$ values.

In Table 3 there is a good agreement between our $\langle x^4 \rangle$ and those of the anharmonic models of M & L. Our $\langle z^4 \rangle$ exhibits the same trend as $\langle z^2 \rangle$; our values are greater than those of M & L. On the other hand, we get a smaller $\langle x^2 z^2 \rangle$ than M & L. Table 5 reports the values of suitable ratios of the moments in four cases. We have included both the experimental limits of error and the uncertainty from column 3 of Table 3 in the limits of error of our moments. The values concerning this work in Table 5 do not significantly deviate from those of Gaussian smearing.

The second moments $\langle x^2 \rangle$ and $\langle z^2 \rangle$ on the same Zn data have been approached by three different methods, those of M & L, K-S, M & P and this work. The method of analysis of M & L and K-S, M & P is parameter fitting, which is basically different from direct analysis (e.g. Vahvaselkä & Kurki-Suonio, 1975). In the parameter-fitting methods explicit expressions can be written for the moments without the uncertainty in determining the saturation points of the moments. The small error limits of the parameters are conditional, they are valid on the condition that the model as a whole with all its parameters yields a correct description of the reality represented by the data. On the contrary, the large error limits of the direct calculation are due to its independence of models. Each quantity is estimated independently on the basis of the data and the nature of the quantity. Thus the large uncertainty of the resulting value of a quantity is to be understood as an indication that any model including this quantity as a parameter would lead to a result

within these limits and as an indication of the uncertainty in the definability of the quantity itself.

References

BACON, G. E. (1972). *Acta Cryst.* A28, 357–358.
BARRON, T. H. K. & MUNN, R. W. (1967). *Acta Cryst.* 22, 170–173.
DAWSON, B. (1975). *Advances in Structure Research by Diffraction Methods*, Vol. 6, edited by W. HOPPE & R. MASON. Oxford: Pergamon Press; Braunschweig: Vieweg.
HOSEMANN, R. & BAGCHI, S. N. (1962). *Direct Analysis of Diffraction by Matter*. Amsterdam: North-Holland.
KURKI-SUONIO, K. (1967). *Ann. Acad. Sci. Fenn. Ser. A6*, 263, 1–7.
KURKI-SUONIO, K. (1968). *Acta Cryst.* A24, 379–390.
KURKI-SUONIO, K. (1971). Proceedings of the Italian Crystallographic Association Meeting, Bari, pp. 31–66.
KURKI-SUONIO, K. (1977a). *Isr. J. Chem.* 16, Nos. 2–3, 115–123.
KURKI-SUONIO, K. (1977b). *Isr. J. Chem.* 16, Nos. 2–3, 132–136.
KURKI-SUONIO, K. & FONTELL, L. (1964). *Ann. Acad. Sci. Fenn. Ser. A6*, 161, 1–12.
KURKI-SUONIO, K. & MEISALO, V. (1967). *Ann. Acad. Sci. Fenn. Ser. A6*, 241, 1–18.
KURKI-SUONIO, K., MERISALO, M. & PELTONEN, H. (1979). *Phys. Scr.* 19, 57–63.
KURKI-SUONIO, K., MERISALO, M., VAHVASELKÄ, A. & LARSEN, F. K. (1976). *Acta Cryst.* A32, 110–115.
KURKI-SUONIO, K. & RUUSKANEN, A. (1971). *Ann. Acad. Sci. Fenn. Ser. A6*, 358, 1–28.
KURKI-SUONIO, K. & SALMO, P. (1971). *Ann. Acad. Sci. Fenn. Ser. A6*, 369, 1–25.
MERISALO, M. & JÄRVINEN, M. (1978). *Philos. Mag.* B37, No. 2, 233–240.
MERISALO, M., JÄRVINEN, M. & KURITTU, J. (1978). *Phys. Scr.* 17, 23–25.
MERISALO, M. & LARSEN, F. K. (1977). *Acta Cryst.* A33, 351–354.
MERISALO, M. & LARSEN, F. K. (1979). *Acta Cryst.* A35, 325–327.
MERISALO, M., PELJO, E. & SOININEN, J. (1978). *Phys. Lett. A*, 67, 80–82.
ROSSMANITH, E. (1977). *Acta Cryst.* A33, 593–601.
SKELTON, E. F. & KATZ, J. L. (1968). *Phys. Rev.* 171, 801–808.
VAHVASELKÄ, A. & KURKI-SUONIO, K. (1975). *Phys. Fenn.* 10, 87–99.
WHITELEY, B., MOSS, G. & BARNEA, Z. (1978). *Acta Cryst.* A34, 130–136.
WILLIS, B. T. M. & PRYOR, A. W. (1975). *Thermal Vibrations in Crystallography*. Cambridge Univ. Press.

Table 5. *Ratios of nuclear distributional moments*

Moments	$\langle x^4 \rangle / \langle x^2 \rangle^2$	$\langle z^4 \rangle / \langle z^2 \rangle^2$	$\langle x^2 z^2 \rangle / \langle x^2 \rangle \langle z^2 \rangle$
Gaussian	3	3	1
This work	3·04 (29)	2·85 (14)	0·99 (11)
M & L anharmonic 1	2·91 (17)	2·32 (45)	1·26 (7)
M & L anharmonic 2	2·99 (16)	2·20 (62)	1·23 (7)